The microscopic approach of sdgIBM-1 and study of the ^{192,190,188}Os isotopes*

Zhang Zhan-Jun[1], Sang Jian-Ping[2], Pan Wu-Ming[3], Liu Yong[1],
([1] *Institute of Particle Physics, Hua-Zhong Normal University, Wuhan 430079,* [2] *Department of Physics, Wuhan University, Wuhan 430072,* [3] *Department of Physics, Hua-Zhong Normal University, Wuhan 430079*)

Abstract From the shell model configurations, valence nucleon effective interactions and fermion E2 transition operator, the sdgIBM-1 Hamiltonian and boson E2 transition operator are derived micoscopically with the help of Dyson boson expansion technique. Spectra and reduced E2 matrix elements are calculated for the ^{192,190,188}Os isotopes. Present theoritical results fit experimental data quite well.

Keywords sdgIBM-1 Hamiltonian, Dyson boson expansion technique, Spectra of ^{192,190,188}Os, Reduced E2 matrix element

1 Introduction

Properties exhibited by the γ-soft Os nuclei have attracted the attention of theoreticians and experimentalists for many years[1~3]. Description of these transition nuclei has been one of the most challenging tasks for collective models of nuclei. Among many models which have been applied to describe these nuclei, the phenomenological interacting boson model (IBM) seems rather satisfactory. In the earlier IBM work, the Os isotopes near ^{190}Os were analyzed by Casten *et al.*[4] as an illustration of O(6) to SU(3) transition. The calculations could produce reasonable agreement with the experimental data. However, there are still more works[5,6], which suggest to include the hexadecapole degrees of freedom. In fact, an extension of the sdIBM to include g bosons has proved to be quite successful indeed in view of Lac and Kuyucak's results[7]. The successful phenomenological description of these transition nuclei invokes us to study its underlying. In the present paper, we extend one of the microscopic approaches of sdIBM[8] to the sdgIBM and apply it to the ^{192,190,188}Os isotopes.

2 Theory

2.1 Fermion description

As the background of present work, the microscopic approach can be found in Ref.(8). The outline is introduced briefly with emphasis focused on the extension.

Assume that there are x valence neutrons and x' valence protons in a nucleus moving respectively in k and k' single-particle orbitals, the shell model configurations, then are

$$(i_1, i_2, \cdots, i_k)^x; \quad (i'_1, i'_2, \cdots, i'_{k'})^{x'} \tag{1}$$

where i stands for three rotationally invariant quantum numbers nlj of a single-particle state.

Let $a^{(n)+}_{im}$, $a^{(n)}_{im}$, $a^{(p)+}_{im}$ and $a^{(p)}_{im}$ denote respectively the creation and annihilation operators of valence neutrons and protons, m the projection of the angular momentum, and let $|0\rangle$ be a closed shell state with $x = x' = 0$, then an arbitrary state vector in the state space of valence nucleons can be expressed as

$$|\psi\rangle = \sum_{\alpha_1 \cdots \alpha_x, \beta_1 \cdots \beta_{x'}} c a^{(n)+}_{\alpha_1} a^{(n)+}_{\alpha_2} \cdots a^{(n)+}_{\alpha_x} a^{(p)+}_{\beta_1} a^{(p)+}_{\beta_2} \cdots a^{(p)+}_{\beta_{x'}} |0\rangle \tag{2}$$

where c is combination constant, and α,β stand for single-particle state (im).

Consider a valence nucleon Hamiltonian which takes a general form

$$H_f = H_f^{(n)} + H_f^{(p)} + H_f^{(np)} \tag{3}$$

*The Project Supported by the National Natural Science Foundation of China
Manuscript received date: 1997-12-13

$$H_{\rm f}^{(\sigma)} = \sum_{\alpha} E_{\alpha}^{(\sigma)} a_{\alpha}^{(\sigma)+} a_{\alpha}^{(\sigma)} + \sum_{\alpha\beta\gamma\delta} P_{\alpha\beta\gamma\delta}^{(\sigma)} a_{\alpha}^{(\sigma)+} a_{\beta}^{(\sigma)+} a_{\gamma}^{(\sigma)} a_{\delta}^{(\sigma)} \quad (\sigma = {\rm n, p}) \tag{4}$$

$$H_{\rm f}^{({\rm np})} = \sum_{\alpha\beta\gamma\delta} P_{\alpha\beta\gamma\delta}^{({\rm np})} a_{\alpha}^{({\rm n})+} a_{\beta}^{({\rm p})+} a_{\gamma}^{({\rm p})} a_{\delta}^{({\rm n})} \tag{5}$$

where $P_{\alpha\beta\gamma\delta}^{(\sigma)}$ and $P_{\alpha\beta\gamma\delta}^{({\rm np})}$ represent matrix elements of the interactions.

For a many fermion system the E2 transition operator is defined as the following

$$T_{2\nu}^{\rm f} = \sum_{\sigma={\rm n,p}} e_2^{(\sigma)} \sum_{i_1 m_1 i_2 m_2} \langle i_1 m_1 | r^2 Y_{2\nu} | i_2 m_2 \rangle a_{j_1 m_1}^{(\sigma)+} a_{j_2 m_2}^{(\sigma)} \tag{6}$$

2.2 Boson description

The fermion description of the system is transformed into an ideal boson description by means of the Dyson mapping. The transformation operator[9] takes the form

$$U = \langle 0 | e^{\frac{1}{2}\sum_{\alpha\beta} A_{\alpha\beta}^{+} a_{\beta} a_{\alpha}} | 0 \rangle \tag{7}$$

then the boson image state $|\psi)$ of a fermion state $|\psi\rangle$ is determined by the operator U,

$$|\psi) = U|\psi\rangle \tag{8}$$

and the counterpart $O_{\rm B}$ in the boson space of an arbitrary fermion operator $O_{\rm f}$ can be determined by the following relation,

$$UO_{\rm f} = O_{\rm B}U \tag{9}$$

Excitation modes describing the low-lying collective states must be low-energetic, thereafter we define the creation operator of Q-bosons in a linear combination of the ideal boson creation operators

$$Q_{r\pi JM}^{(\sigma)+} = \sum_{\alpha\le\beta} x_{\alpha\beta}^{(r\pi JM)} A_{\alpha\beta}^{(\sigma)+} \tag{10}$$

where r stands for the ordering of energy of Q-boson, π and J represent parity and angular momentum respectively, $x_{\alpha\beta}^{(r\pi JM)}$ is the structure constant. According to the dynamic properties[8], $x_{\alpha\beta}^{(r\pi JM)}$ and the energies of Q-bosons can be determined. The lowest-energy Q-boson of different angular momentums would be suitable for describing the low-lying collective states, so this kind of Q-bosons are taken as phenomenological bosons

$$s^{(\sigma)} = Q_{0+00}^{(\sigma)}; \quad d_{\nu}^{(\sigma)} = Q_{0+2\mu}^{(\sigma)}; \quad g_{\nu}^{(\sigma)} = Q_{0+4\nu}^{(\sigma)} \tag{11}$$

Once the s, d and g bosons have been determined, one can arrive at the most general Hamiltonian with all possible one-body terms and two-body interactions, and boson E2 transition operator as well in the sdgIBM-2,

$$h_{\rm sdg} = h_{\rm sdg}^{({\rm n})} + h_{\rm sdg}^{({\rm p})} + h_{\rm sdg}^{({\rm np})} \tag{12}$$

$$\begin{aligned} T_{2\nu} = \sum_{\sigma={\rm n,p}} e_2^{(\sigma)} [& x_{02}^{(\sigma)} (s^{(\sigma)+} \tilde{d}^{(\sigma)} + d^{(\sigma)+} \tilde{s}^{(\sigma)})_{2\nu} + x_{22}^{(\sigma)} (d^{(\sigma)+} \tilde{d}^{(\sigma)})_{2\nu} \\ & + x_{24}^{(\sigma)} (d^{(\sigma)+} \tilde{g}^{(\sigma)} + g^{(\sigma)+} \tilde{d}^{(\sigma)})_{2\nu} + x_{44}^{(\sigma)} (g^{(\sigma)+} \tilde{g}^{(\sigma)})_{2\nu}] \\ \equiv & \sum_{\sigma={\rm n,p}} e_2^{{\rm B}(\sigma)} Q_{2\nu}^{(\sigma)} \end{aligned} \tag{13}$$

where the coefficients $\{x^{(\sigma)}\}$ can be obtained after the Dyson boson expansion, $Q_{2\nu}^{(\sigma)}$ is boson quadrupole operator,

$$\begin{aligned} Q_{2\nu}^{(\sigma)} = & (s^{(\sigma)+} \tilde{d}^{(\sigma)} + d^{(\sigma)+} \tilde{s}^{(\sigma)})_{2\nu} + \chi_1^{(\sigma)} (d^{(\sigma)+} \tilde{d}^{(\sigma)})_{2\nu} \\ & + \chi_2^{(\sigma)} (d^{(\sigma)+} \tilde{g}^{(\sigma)} + g^{(\sigma)+} \tilde{d}^{(\sigma)})_{2\nu} + \chi_3^{(\sigma)} (g^{(\sigma)+} \tilde{g}^{(\sigma)})_{2\nu} \end{aligned} \tag{14}$$

Comparing Eq.(13) with Eq.(14), we get

$$e_2^{{\rm B}(\sigma)} = e_2^{(\sigma)} x_{02}^{(\sigma)}, \tag{15}$$

$$\chi_1^{(\sigma)} = \frac{x_{22}^{(\sigma)}}{x_{02}^{(\sigma)}};\quad \chi_2^{(\sigma)} = \frac{x_{24}^{(\sigma)}}{x_{02}^{(\sigma)}};\ ,\ \chi_3^{(\sigma)} = \frac{x_{44}^{(\sigma)}}{x_{02}^{(\sigma)}} \tag{16}$$

where $e_2^{\mathrm{B}(\sigma)}$ ($\sigma = \mathrm{n}, \mathrm{p}$) is boson effective charge.

The dimensionality of sdgIBM-2 space is much bigger than that of sdgIBM-1 space. In order to make the problem easier, it is convenient to take advantage of the full-symmetry approximation denoted by the maximum F-spin quantum number, $F_{\max} = \frac{1}{2}(N_\mathrm{n} + N_\mathrm{p})$, where N_n, N_p are neutron, proton boson number respectively. After the full-symmtry approximation, one can obtain the most general Hamiltonian[10,11] and E2 transition operator in the sdgIBM-1,

$$\hat{h}_{\mathrm{sdg}} = h_{\mathrm{sd}} + h_\mathrm{g} + h(\mathrm{sd};\mathrm{g}) \tag{17}$$

$$\hat{T}_{2\nu} = e_2^\mathrm{B} Q_{2\nu} \tag{18}$$

where $Q_{2\nu}$ takes the same form as $Q_{2\nu}^{(\sigma)}$,

$$e_2^\mathrm{B} = \frac{N_\mathrm{n}}{N_\mathrm{n}+N_\mathrm{p}} e_2^{\mathrm{B(n)}} + \frac{N_\mathrm{p}}{N_\mathrm{n}+N_\mathrm{p}} e_2^{\mathrm{B(p)}} \tag{19}$$

Coefficients in the quadrupole operator $Q_{2\nu}$ are determined, i.e.

$$\chi_i = \frac{N_\mathrm{n} e_2^{\mathrm{B(n)}} \chi_i^{(\mathrm{n})} + N_\mathrm{p} e_2^{\mathrm{B(p)}} \chi_i^{(\mathrm{p})}}{N_\mathrm{n} e_2^{\mathrm{B(n)}} + N_\mathrm{p} e_2^{\mathrm{B(p)}}}, \qquad i = 1,2,3 \tag{20}$$

Up to now, the sdgIBM-1 Hamiltonian and boson E2 transition operator have already been obtained microscopically. Therefore, we can study the E2 or other properties in the framework of sdgIBM-1.

3 Application of the extended approach and discussions

Now we apply the microscopic approach to the Os isotopes. For ^{192,190,188}Os there are 6 proton-holes in the $50 \sim 82$ major shell and $10 \sim 14$ neutron-holes in the $82 \sim 126$ major shell. As inputs of the extended approach, the single particle energies we adopted[12] are as followings: (in MeV)

$E_{2f_{7/2}} = 0.00$, $E_{3p_{3/2}} = 0.30$, $E_{1h_{9/2}} = 2.20$, $E_{2f_{5/2}} = 3.50$, $E_{1i_{13/2}} = 3.60$, $E_{3p_{1/2}} = 4.60$; $E_{1g_{7/2}} = 0.00$, $E_{1f_{5/2}} = 0.32$, $E_{1h_{11/2}} = 2.32$, $E_{2d_{3/2}} = 2.84$, $E_{3s_{1/2}} = 3.21$.

The valence nucleon effective interactions, also inputs of the approach, are taken as the following type. The interactions between alike nucleons consist of pairing force, quadrupole pairing force and quadrupole-quadrupole force, the neutron-proton interaction is of quadrupole-quadrupole type. The interaction strength parameters are labeled as $g_0^{(\sigma)}$, $G_2^{(\sigma)}$, $\kappa^{(\sigma)}$ ($\sigma = \mathrm{n}, \mathrm{p}$) and κ_{np} accordingly. Their values are listed in Table 1. The fermion effective charges for ^{192,190,188}Os isotopes are listed in Table 2.

Table 1 The parameters of valence nucleon effective interaction. (keV)

Nucleus	$g_0^{(n)}$	$G_2^{(n)}$	$\kappa^{(n)}$	$g_0^{(p)}$	$G_2^{(p)}$	$\kappa^{(p)}$	κ_{np}
^{192}Os	40.0	45.0	12.0	47.0	61.0	23.0	5.0
^{190}Os	40.0	43.0	12.0	47.0	63.0	23.0	5.0
^{188}Os	40.0	43.0	12.0	47.0	66.0	23.0	6.0

Table 2 Neutron (proton) effective charge $e_2^{(n)}$ ($e_2^{(p)}$) and the coefficents of boson E2 transition operator for ^{192,190,188}Os

Nucleus	$e_2^{(n)}$	$e_2^{(p)}$	e_2^B	χ_1	χ_2	χ_3
^{192}Os	3.20e	3.60e	0.149eb	0.434	1.177	1.030
^{190}Os	3.00e	3.20e	0.138eb	0.443	1.182	1.036
^{188}Os	2.70e	3.00e	0.126eb	0.447	1.183	1.034

In the framework of the extended approach mentioned above, the sdgIBM-1 Hamiltonian and boson E2 transition operator have been obtained. 32 coefficients in total in the Hamiltonian and 4 coefficients including boson effective charge in the E2 transition operator are calculated simultaneously. The coefficients of E2 transition operator are listed in Table 2. Boson effective charges determined microscopically are close to those adopted phenomenologically in Ref.[7].

The spectra in the microscopic calculations for ^{192,190,188}Os exhibit almost the same

level structures, as an example shown in Fig.1. The energies of low-lying states in the ground band are reproduced quite well, while in the sidebands, the fitting is not as good as that in the ground band. But generally speaking, the fitting between the present calculation and the experiment is satisfactory. In the microscopic sdIBM-1 approach all the theoretical energy levels are much higher than experimental ones, especially in the sidebands. After the extension to include g bosons the improvement has been achieved. For all the energy levels in the Fig.1, the mean deviation in the sdgIBM-1 ($\approx$ 0.198MeV) is almost half of that ($\approx$ 0.336 MeV) in the sdIBM-1. The present theoretical spectrum has also shown major characters near O(6) limit in sdIBM-1, such as staggering in the quasi-γ band and quadruplet 6_1^+, 4_2^+, 3_1^+ and 0_2^+. So one can think although the effects of g bosons are really important to some specific properties, the main components in the wavefunctions are still those near O(6) limit in sdIBM-1.

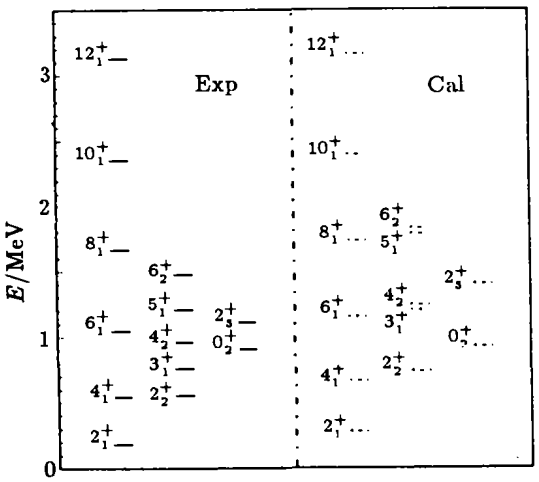

Fig.1 Spectra obtained from microscopic calculation and experimental data for ^{190}Os

Table 3 Absolute values of reduced E2 matrix elements of ^{192}Os (in eb). The experimental data are taken from Ref.[13]

$J_i^+ \to J_f^+$	Exp	Cal	$J_i^+ \to J_f^+$	Exp	Cal
$2_1^+ \to 0_1^+$	1.457 ± 0.018	1.404	$6_2^+ \to 6_1^+$	$1.49(^{+0.30}_{-0.20})$	1.702
$4_1^+ \to 2_1^+$	$2.115(^{+0.038}_{-0.044})$	2.309	$6_2^+ \to 4_2^+$	$2.09(^{+0.13}_{-0.17})$	2.581
$6_1^+ \to 4_1^+$	$2.93(^{+0.10}_{-0.08})$	2.995	$6_2^+ \to 4_1^+$	0.067 ± 0.076	0.164
$8_1^+ \to 6_1^+$	$3.58(^{+0.17}_{-0.15})$	3.508	$4_3^+ \to 4_2^+$	1.19 ± 0.22	1.585
$2_2^+ \to 2_1^+$	$1.224(^{+0.030}_{-0.016})$	1.575	$4_3^+ \to 3_1^+$	$1.63(^{+0.20}_{-0.36})$	1.707
$2_2^+ \to 0_1^+$	$0.425(^{+0.008}_{-0.014})$	0.040	$4_3^+ \to 2_2^+$	$0.79(^{+0.12}_{-0.14})$	0.009
$2_2^+ \to 4_1^+$	$0.35(^{+0.12}_{-0.07})$	0.171	$4_3^+ \to 2_1^+$	$0.113(^{+0.064}_{-0.046})$	0.080
$0_2^+ \to 2_1^+$	$0.066(^{+0.012}_{-0.013})$	0.472	$2_1^+ \to 2_1^+$	1.21 ± 0.18	0.729
$0_2^+ \to 2_2^+$	$0.449(^{+0.044}_{-0.056})$	0.418	$4_1^+ \to 4_1^+$	$0.73(^{+0.15}_{-0.10})$	0.980
$4_2^+ \to 4_1^+$	$1.35(^{+0.10}_{-0.08})$	1.603	$6_1^+ \to 6_1^+$	$1.16(^{+0.24}_{-0.34})$	1.223
$4_2^+ \to 2_2^+$	1.637 ± 0.050	1.806	$8_1^+ \to 8_1^+$	$1.31(^{+0.48}_{-0.66})$	1.430
$4_2^+ \to 2_1^+$	$0.125(^{+0.018}_{-0.010})$	0.084	$10_1^+ \to 10_1^+$	(-2.3-0.4)	1.626
$4_2^+ \to 6_1^+$	$0.40(^{+0.20}_{-0.18})$	0.231	$2_2^+ \to 2_2^+$	0.98 ± 0.10	0.480

Table 4 Absolute values of reduced E2 matrix elements of ^{190}Os (in eb). The experimental data are taken from Refs.[14,15]

$J_i^+ \to J_f^+$	Exp	Cal	$J_i^+ \to J_f^+$	Exp	Cal
$2_1^+ \to 0_1^+$	1.539 ± 0.013	1.483	$6_2^+ \to 6_1^+$	1.766 ± 0.184	1.785
$4_1^+ \to 2_1^+$	2.366 ± 0.042	2.433	$6_2^+ \to 4_2^+$	2.598 ± 0.156	2.723
$6_1^+ \to 4_1^+$	2.970 ± 0.515	3.152	$6_2^+ \to 4_1^+$	0.194 ± 0.090	0.210
$8_1^+ \to 6_1^+$	3.712 ± 0.105	3.714	$4_3^+ \to 4_2^+$	1.587 ± 0.113	1.640
$2_2^+ \to 2_1^+$	1.095 ± 0.030	1.577	$4_3^+ \to 3_1^+$	$1.543(^{+0.091}_{-0.340})$	1.770
$2_2^+ \to 0_1^+$	0.456 ± 0.012	0.077	$4_3^+ \to 2_2^+$	0.775 ± 0.065	0.062
$0_2^+ \to 2_2^+$	0.387 ± 0.032	0.533	$4_3^+ \to 2_1^+$	0.052 ± 0.006	0.107
$0_2^+ \to 2_1^+$	0.118 ± 0.011	0.514	$4_3^+ \to 4_1^+$	≈ 0.199	0.135
$4_2^+ \to 4_1^+$	1.439 ± 0.031	1.636	$2_1^+ \to 2_1^+$	1.253 ± 0.396	0.975
$4_2^+ \to 2_2^+$	1.871 ± 0.040	1.894	$2_2^+ \to 2_2^+$	1.187 ± 0.528	0.665
$4_2^+ \to 2_1^+$	0.202 ± 0.007	0.112			

In the theoretical spectrum, 6_1^+, 4_2^+ and 3_1^+ looks as a group while 4_1^+ and 2_2^+ as another one, and 0_2^+ lies between those two groups. This phenomenon indicates the admixture of some components of U(5) limit in 0_2^+ state. One can confirm this point of view through the analysis of $\langle 0_2^+||T(E2)||2_1^+\rangle$. The Os isotopes near ^{190}Os were analyzed by Casten *et al.*[4] as an illustration of O(6) to SU(3) transition in the sdIBM. $\langle 0_2^+||T(E2)||2_1^+\rangle$ in either the O(6) limit or the SU(3) limit should be zero while in U(5) limit not. The calculated reduced E2 matrix elements are listed in Tables 3 $\sim$ 5 compared with the experimental data. From Tables 3 $\sim$ 5 one can find the experimental $\langle 0_2^+||T(E2)||2_1^+\rangle$s are really very small. However, the calculated $\langle 0_2^+||T(E2)||2_1^+\rangle$s are nearly 5 $\sim$ 7 times of those experimental ones, it reflects the affection of components of U(5) limit. However, such affection also exists in the microscopic sdIBM-1 and is not decreased due to the extension. Maybe some other degrees of freedom are needed in describing 0_2^+ such as the influence of d' bosons.

Table 5 Absolute values of reduced E2 matrix elements of ^{188}Os (in eb). The experimental data are taken from Refs.[15,16]

$J_i^+ \to J_f^+$	Exp	Cal	$J_i^+ \to J_f^+$	Exp	Cal
$2_1^+ \to 0_1^+$	1.584 ± 0.022	1.653	$4_2^+ \to 2_1^+$	0.283 ± 0.018	0.182
$4_1^+ \to 2_1^+$	2.646 ± 0.057	2.627	$6_2^+ \to 6_1^+$	1.442 ± 0.406	1.759
$6_1^+ \to 4_1^+$	3.314 ± 0.109	3.330	$6_2^+ \to 4_2^+$	2.456 ± 0.274	2.769
$8_1^+ \to 6_1^+$	3.950 ± 0.329	3.896	$6_2^+ \to 4_1^+$	0.127 ± 0.025	0.315
$2_2^+ \to 2_1^+$	0.866 ± 0.023	1.440	$4_3^+ \to 4_2^+$	1.643 ± 0.246	1.681
$2_2^+ \to 0_1^+$	0.483 ± 0.010	0.145	$4_3^+ \to 2_2^+$	0.837 ± 0.149	0.183
$0_2^+ \to 2_1^+$	0.077 ± 0.029	0.513	$2_1^+ \to 2_1^+$	1.517 ± 0.330	1.476
$4_2^+ \to 4_1^+$	1.098 ± 0.090	1.560	$2_2^+ \to 2_2^+$	1.319 ± 0.330	1.081
$4_2^+ \to 2_2^+$	1.775 ± 0.113	1.944			

The experimental results show that the in-band transition is strong while the interband transition weak. The calculated results, given in Tables 3 $\sim$ 5, show that such features of transition properties for ^{192,190,188} Os are well reproduced by the present microscopic calculations with a few exceptions. Nevertheless we notice that the present results are much similar to those of phenomenological sdgIBM-1 study by Lac *et al.*[7]. It means that the resulting wavefunctions describe the excited states well.

In summary, the achievement in calculation of spectra and the reduced E2 matrix elements in the Os isotopes indicates the success of the microscopic approach. The present extension has improved the fitting of spectra and the reduced E2 matrix elements between the calculation and the experimental data. At last, it is worth to point out that the extension has provide a reasonable underlying of the phenomenological sdgIBM-1.

References

1 Ansari A. Phys Rev, 1988, C38:323
2 Chiang H C, Hsieh S T, Kuo T T S. Phys Rev, 1988, C38:2453
3 Boeglin W, Egelhof P, Sick P *et al.* Nucl Phys, 1988, A477:399
4 Casten R F, Warner D D. Rev Mod Phys, 1988, 60:389
5 Ansari A. Phys Rev, 1988, C38:953
6 Todd Baker F, Sethi A, Penumetcha V. Phys Rev, 1985, C32:2212
7 Lac V S, Kuyucak S. Nucl Phys, 1992, A539:418
8 Yang Z S, Liu Y, Qi H. Nucl Phys, 1984, A421:297
9 Usui T. Progr Theor Phys, 1960, 23:787
10 Zhang Z J, Liu Y, Sang J P. Chin J Nucl Phys, 1995, 17:318
11 Liu Y, Shi Z Y, Dan H J *et al.* Chin J Nucl Phys, 1995, 17:194
12 Liu Yong. Ph D Thesis, Beijing University, 1984
13 Wu C Y. Ph D Thesis, University of Rochester, 1983
14 Singh B. Nucl Data Sheets, 1990, 61:243
15 Raghavan P. At Data Nucl Data Tables, 1989, 42:189
16 Singh B. Nucl Data Sheets, 1990, 59:133